The Cryosphere Discuss., 5, 3259–3289, 2011
www.the-cryosphere-discuss.net/5/3259/2011/
doi:10.5194/tcd-5-3259-2011

The Cryosphere Discussions

Albedo of the ice-covered Weddell and Bellingshausen Sea

A. I. Weiss, J. C. King, T. A. Lachlan-Cope, and R. S. Ladkin

British Antarctic Survey, National Environment Research Council, High Cross, Madingley Road, Cambridge, CB3 0ET, UK

Received: 13 October 2011 – Accepted: 16 November 2011 – Published: 30 November 2011

Correspondence to: A. I. Weiss (aiw@bas.ac.uk)

Published by Copernicus Publications on behalf of the European Geosciences Union.

Abstract

This study investigates the surface albedo of the sea ice areas adjacent to the Antarctic Peninsula during the austral summer. Aircraft measurements of the surface albedo which were conducted in the sea ice areas of the Weddell and Bellingshausen Sea show significant differences between these two regions. The averaged surface albedo varied between 0.13 and 0.81. The ice cover of the Bellingshausen Sea consisted mainly of first year ice and the sea surface showed an averaged sea ice albedo of $\overline{\alpha_i} = 0.64 \pm 0.2$ (±standard deviation). The mean sea ice albedo of the pack ice area in the Western Weddell Sea was $\overline{\alpha_i} = 0.75 \pm 0.05$. In the Southern Weddell Sea, where new, young sea ice prevailed, a mean albedo value of $\overline{\alpha_i} = 0.38 \pm 0.08$ was observed. Relatively warm open water and thin, newly formed ice had the lowest albedo values, whereas relatively cold and snow-covered pack ice had the highest albedo values. All sea ice areas consist of a mixture of a large variability of different sea ice types. An investigation of commonly used parameterizations of albedo as a function of surface temperature in the Weddell and Bellingshausen Sea ice areas showed that the albedo parameterizations don't work well in particular for areas with new, young ice. We determined typical linear temperature-albedo functions for three sea ice areas adjacent to the Antarctic Peninsula, which are reflecting the differences in the mixture of ice age, thickness and sea ice surface cover.

1 Introduction

The albedo α is defined as the ratio of shortwave outgoing Sw_{up} to shortwave incoming radiation Sw_{down}. In polar regions sea ice exerts a strong control on the sea surface albedo. Trends in the satellite-derived Antarctic sea ice concentrations (1979–2002) show a clear decrease in the Bellingshausen and Western Weddell Sea by about 4–10 % per decade (Liu et al., 2004). This may have been caused by a temperature change, as since the 1950s a major warming trend has been observed in annual mean temperature on the western side of the Antarctic Peninsula of about 0.56 °C per decade. The largest statistically-significant temperature increase on the eastern side of the Antarctic Peninsula has occurred during summer (Turner et al., 2006). In order to investigate effects of such a sea ice decrease in the Antarctic on the climate system, climate model studies have to be performed, which require accurate specification or parameterization of the albedo. However, the Antarctic is a region where there is a large spread in the predictions of future climate between different models (Bracegirdle et al., 2008). One reason for this might be that the Antarctic sea ice zone remains one of the least known regions on Earth and only few direct observations of the albedo in the Antarctic sea ice zone exist so far (e.g. Predoehl and Spano, 1965; Allison et al., 1993; Pirazzini, 2004; Zhou et al., 2007; Vihma et al., 2009; Brandt et al., 2005).

To deepen our understanding of the albedo of Antarctic sea ice areas, we have analyzed aircraft-based field measurements conducted by the British Antarctic Survey in the austral summers of 2006/2007 and 2007/2008. Our study has three main goals. First, we aim to determine regional differences in the sea surface albedo between the Bellingshausen Sea and the Western Weddell Sea. We then attempt to explain these differences in terms of sea ice parameters that influence the sea surface albedo, such as the average percentage of prevailing sea ice type, sea ice concentration and by the surface temperature. In order to describe the surface albedo in the sea ice area representative of the non-homogenous sea surface, area-averaged albedo values of the sea surface need to be known. Area-averaged albedo values of the non-homogenous sea ice area can be a composite of albedo values of open water in leads and polynyas, bare ice or various kinds of snow-covered ice of different age. Therefore, the second goal of this study is to determine typical area-averaged surface albedo values as well as averaged sea ice albedo values which are representative of sea ice areas adjacent to the Antarctic Peninsula in summer. Most climate and numerical weather prediction models cannot take into account all of the factors that influence the albedo in the sea ice area. The main reason for this is that not all necessary information is available in a model as input parameters for a complex albedo parameterization. In fact, very often the albedo

TCD
5, 3259–3289, 2011

parameterizations in numerical models are relatively simple and assume a constant value for a model grid cell or parameterize the sea ice albedo solely with the surface temperature. The surface temperature is not a good physical predictor for the albedo of the ice-covered sea, but the temperature is an input variable which is available in most models. These parameterizations uses the fact that the surface temperature acts as a proxy for physical parameters which influences the radiative properties of the ice-covered sea surface, such as thickness of the ice, snow cover, snow grain size and amount of brine in the sea ice. Up to now, sea ice albedo parameterization schemes were largely determined and validated with data sets which were collected in the Arctic (e.g. Curry et al., 2001) and little is known about how well those parameterization schemes perform for Antarctic sea ice areas. Therefore, the third goal of this study is to address the relation between temperature and albedo in Antarctic sea ice zones. We investigate whether commonly-used albedo parameterizations, which use the temperature as the sole input forcing parameter, are appropriate to describe the albedo of the sea ice areas in the Western Weddell Sea and the North-Eastern Bellingshausen Sea in summer.

2 Methods

2.1 Observational area

Airborne observations of sea surface albedo in the Antarctic were carried out during two austral summer measurement campaigns. The first campaign took place during February and March 2007 and the second during January and February 2008. Measurements were made using an instrumented DHC6 Twin Otter aircraft operated by the British Antarctic Survey. All flights started from Rothera Research Station on Adelaide Island (67.6° S, 68.1° W). During these two campaigns the sea surface albedo was measured in the area of the Western Weddell Sea (around 65° S–75° S, 55° W–61° W) and in the North-Eastern Bellingshausen Sea (68.6° S–69.9° S, 70.8° W–75.6° W).

TCD
5, 3259–3289, 2011

Figure 1 shows a map of the Antarctic Peninsula with the flight tracks (black lines) of the 2007 and 2008 campaigns which form the basis of this study. The albedo measurements, which are presented in this study, were mainly conducted over a compact ice-covered sea surface.

The amount of sea ice is determined by the sea ice mass balance, i.e. by the amount of sea ice which is produced or melted. In the Antarctic there is a strong interannual and spatial variation of the sea ice mass balance. The melt season is driven mainly by the solar radiation and the onset of melt occurs in the austral spring season. Main factors which influences the sea ice mass balance are the air and sea surface temperature, heat fluxes at the top, bottom and boundaries of the sea ice, sea ice brine volume, snow cover and thickness, the sea ice albedo, the movement of ice by wind and ocean current and the salinity of the sea, because it influences the freezing point of sea water. The salinity varies between the Weddell and the Bellingshausen Sea. An overview about oceanic parameters in the Weddell Sea can be found e.g. by Nicholls et al. (2001, 2008). The typical regional surface salinity in the southern part of the Western Weddell Sea is around 33.5 to 34.1 which results in a freezing point of $T_s = -1.84$ to $-1.89\,^{\circ}$C. Oceanographic measurements in the Bellingshausen Sea (Jenkins and Jacobs, 2008) showed that the surface salinity in this sea ice area varies around 32.7 to 33.5 which leads to a freezing point between $T_s = -1.79$ and $-1.84\,^{\circ}$C.

2.2 Aircraft instrumentation

The aircraft was instrumented with upward- and downward-facing pyranometers (Epplev, PSP) to measure shortwave radiation, and upward- and downward facing pyrgeometers (Eppley, PIR) to measure longwave radiation. The radiometers have a 2π viewing angle. However, the irradiance which is detected by the upward directed pyranometer is controlled by the cosine of the solar zenith angel. The cosine response of the PSP pyranomenters is 1 % for 0–70° from zenith (which can be assumed for the data of this study) and 3 % for 70–80° from zenith. The broadband albedo (in this study simply called albedo) of the surface was determined from the ratio of the upward- and downward-facing pyranometer data. The pyranometers provides an albedo value in the wavelength range of 0.285 to 2.8 µm. The logging frequency of all radiometers was 10 Hz. Raw data from the upward-facing pyranometer was corrected for aircraft attitude variations after Bannehr and Glover (1991). For the determination of the aircraft position and attitude we used data of a JAVAD AT4 four-antenna GPS system. This GPS system gives all three components of aircraft position, attitude and velocity at a rate of 20 Hz. The resolution of the pyranometers lies in the range of 0.5 W m^{-2} and they measure with an estimated accuracy of 3 %. The downward-facing radiation sensors were mounted on the underside of the aircraft together with a downward-looking video camera and a Heimann KT 19.82 infrared thermometer (IRT). The lens of the IRT provides a field of view of the sea surface of 4.42 m (diameter) at a flight height of 100 m. The IRT sensor on the aircraft enabled the recording of the sea surface temperature along the flight tracks. In order to minimize errors due to non-optimal working temperatures of the IRT on the aircraft, the sensor was insulated. The IRT detector has a spectral sensitivity in the range of 8 to 14 µm, i.e. the sensitivity range lies in a water vapor window of the atmosphere. In this spectral range the transmission of the atmosphere for infrared wavelengths is relatively high. To reduce the remaining error due to absorption and emission by atmospheric gases, we conducted the observations at relatively low flight levels at heights around 20 to 80 m. We account for remaining emission and absorption effects by the intervening atmosphere between aircraft and surface by using a constant correction factor, as described by Burns et al. (2000). Additional atmospheric variables such as temperature, wind, humidity, as well as turbulent fluxes of heat and momentum were measured with a NOAA/ARA BAT probe, a fast response temperature sensor and a Buck Research 1011C cooled-mirror dew point hygrometer. Most of the atmospheric aircraft instrumentation was tested in the Antarctic in a field campaign in 2006. A detailed description of the instrumental set-up on the Twin Otter aircraft is given by King et al. (2008) and Weiss et al. (2011).

TCD
5, 3259–3289, 2011

2.3 Determination of sea ice concentration

To obtain information about the sea ice concentration C_{ice} we analyzed measurements from the IRT, the pyranometers and the video camera. The sea ice concentration was calculated by discriminating between ice and open water using thresholds for surface temperature (freezing point) and albedo. To determine the threshold for temperature, i.e. the freezing point, we assessed the typical salinity of the surface sea water for the three main sea ice areas: we assumed a mean surface sea water salinity of 34.1 for the Weddell Sea pack ice region and estimated the freezing point of the sea water to be $T_f = -1.87\,^{\circ}$C. For the southern part of the Western Weddell Sea, in the Ronne Polynya region, we assumed a mean salinity of 34.5 and estimated the freezing point to be $T_f = -1.89\,^{\circ}$C and for the North-Eastern part of the Bellingshausen Sea we assumed a mean value of the salinity of 33.1 and of the sea water freezing point of $T_f = -1.81\,^{\circ}$C. The freezing points were used to distinguish between ice and open water in combination with an albedo value threshold of $\alpha_w \leq 0.07$ for open water and of $\alpha_i > 0.07$ for the ice-covered sea surface. With this algorithm we determined from the high resolution 10 Hz data remotely the sea ice concentration of each flight. This method gives only an approximation about the sea ice concentration because we use a mean salinity value and moreover, the field of view of the pyranometers and the IRT are different as described in Sect. 2.2. Due to the fact that the field of view of the IRT is smaller than that of the pyranometers an over- or underestimation of the irradiance for the sea ice area the IRT is detecting can result. This would be the case in particular for sea ice areas which show a strong heterogeneous sea surface due to a mixture of water or thin dark ice and solid white sea ice. However, most of our measurements presented in this study were conducted at low surface temperatures and over relatively compact sea ice with a small water fraction and we combined additionally video footage to the radiation measurements, which allows often distinguishing between thin dark ice and open water patches.

TCD

5, 3259–3289, 2011

3 Observations and results

3.1 Sea ice characteristics

The ice-covered sea surface in the North-Eastern Bellingshausen Sea in February 2007 comprised a mixture of different first year sea ice types such as thin white ice, medium and thick first year ice and snow-covered first year ice. By contrast, during the 2008 observing campaign, this region was almost ice-free. The floe size of the first year ice, which we observed in February 2007, ranged typically from less than 20 m across to up to medium floes with diameters ranging from 100 to 500 m. between the floes we observed slush and frazil ice and/or nilas and icebergs. Corresponding to this wide range of surface types, the sea surface in the North-Eastern Bellingshausen Sea showed a large range of albedo and surface temperature values in 2007. A typical example of the sea ice conditions in the North-Eastern Bellingshausen Sea and the corresponding observed albedo and surface temperature values is given in the left panels of Fig. 2. The upper left panel displays a picture of the ice conditions that we observed on the 26 February 2007. The lower left panel shows the high resolution data (10 Hz) of sea surface albedo as a function of sea surface temperature during that flight over sea ice. The albedo values show a tendency to be inversely related to the surface temperature: lowest albedo values were around $\alpha_{min} = 0.06$ and correspond to surface temperatures of open water. Highest albedo values reach more than $\alpha_{max} \geq 0.8$ and correspond to surface temperatures in the range of about $-9.0\,^{\circ}\mathrm{C} < T_s \leq -6.0\,^{\circ}\mathrm{C}$. These high albedo values at low surface temperatures are characteristic of snow-covered sea ice (e.g. Brandt et al., 2005). The averaged surface temperature of the mixture of sea ice and open water of this flight mission was $\overline{T_s} = -2.3\,^{\circ}\mathrm{C}$ corresponding to an averaged albedo of $\overline{\alpha} = 0.16$. The averaged sea ice temperature was $\overline{T_i} = -2.91\,^{\circ}\mathrm{C}$ and the sea ice had an averaged albedo of $\overline{\alpha_i} = 0.25$.

In the Western Weddell Sea we deduced from visual observations that the fast ice adjacent to the Larsen Ice Shelf can be characterized mainly as snow-covered

TCD
5, 3259–3289, 2011

multi-year pack ice. The main reason for sea ice remaining over more than one season in the Western Weddell Sea is the prevailing ocean current. In the Central Weddell Sea the clockwise-directed Weddell Gyre traps the sea ice along the east coast of the Antarctic Peninsula. The Weddell Gyre transports the sea ice relatively slowly. During both campaigns, in 2007 and 2008, we observed that the pack ice in the Western Weddell Sea seldom forms a closed cover, but polynyas and leads were present. Leads and polynyas persist as open water, but when temperatures drop below the freezing point grease ice, nilas and grey ice form rapidly on their surface. The two panels in the middle of Fig. 2 display a typical picture of the Western Weddell Sea pack ice area (16 February 2007) and the albedo as a function of the sea surface temperature. Lowest albedo values of $\alpha_{min} = 0.07$ corresponded to sea surface temperatures of $T_s = -1.91\,^{\circ}\mathrm{C}$ near the freezing point of sea water. Visually we observed hardly any patches of open water but very thin, dark ice during this flight. Largest albedo values of more than $\alpha_{max} \geq 0.8$ were observed at surface temperatures around $T_s = -8.0\,^{\circ}\mathrm{C}$ which we visually allocate to snow-covered pack ice. The reason why snow-covered sea ice has a higher albedo than snow-free ice is due to the fact that snow consists of a large number of grains which increase the scattering of the incoming radiation. Fine grained snow, which is often relatively cold snow, is more likely to scatter radiation back than snow of larger grains, which is often relatively warm snow. The grain size radius for new snow is in the order of 20–100 µm, for fine grained older snow in the order of 100–300 µm and 1.0–1.5 mm for old now near the melting point (Wiscombe and Warren, 1980). Wiscombe and Warren (1980) showed with a radiative transport model that the albedo decreases as the grain size increases. This is due to the fact that larger grains are both more absorptive and more forward scattering. The averaged surface temperature during this flight mission was $\overline{T_s} = -6.93\,^{\circ}\mathrm{C}$ corresponding to an averaged albedo of $\overline{\alpha} = 0.76$.

In the southern part of the Western Weddell Sea a polynya persists off the front of the Ronne Ice Shelf, known as the Ronne Polynya. The Ronne Polynya is the result of the prevailing wind in this area which is a mostly southerly to south-easterly wind, resulting form cold air draining from the continent being forced northwards by the mountains of the Antarctic Peninsula. This prevailing wind direction together with the ocean current, which follows the barrier of the Ronne Ice Shelf westwards, makes this polynya a characteristic feature of this part of the Weddell Sea. The size of the Ronne Polynya varied between our flight missions because new, young and grey ice formed rapidly on open water in this area when the air temperatures dropped below the freezing point, in particular during cold air outflows from the Ronne Ice Shelf. A picture of the new, young and grey ice-covered polynya area, taken on 25 February 2007, is shown in the right top panel of Fig. 2. The lower right panel displays the relation between surface albedo and surface temperature. The surface albedo ranged from $\alpha_{min} = 0.07$ up to $\alpha_{max} = 0.9$ within a surface temperature range of $T_s = -1.5\,^{\circ}$C to $T_s = -9.7\,^{\circ}$C. The averaged surface temperature was $\overline{T_s} = -6.31\,^{\circ}$C with an averaged surface albedo of $\overline{\alpha} = 0.38$. Close to the Ronne Ice Shelf we measured higher surface temperatures and lower albedo values. 50–100 km away from the Ronne Ice Shelf the prevailing sea ice became considerably thicker and snow-covered, showing lower surface temperatures and the surface albedo increased in this area up to more than $\alpha \geq 0.8$. This is in agreement with ship measurements of the albedo of Brandt et al. (2005).

All three examples in Fig. 2 show that the sea ice albedo increases with a decrease in surface temperature, but it can also be seen that a certain albedo value can occur at various temperatures. The large scatter indicates that the temperature is not directly linked to the albedo. The surface temperature is acting as a proxy for some of the physical factors which influences the albedo of the ice-covered sea, but there are also factors which depend not directly on the temperature. Previous experimental and theoretical model studies investigated how factors like solar zenith angle and cloud cover (e.g. Vashisth, 2005; Grenfell and Perovich, 1984), wavelength (e.g. Grenfell et al., 1994), salinity (Perovich and Grenfell, 1981) and snow cover (e.g. Brandt et al., 2005), among other factors influence the radiative properties of sea ice. The examples in Fig. 2 suggest that the albedo is strongly controlled by the ice thickness and snow cover and that the temperature is a good proxy for these parameters. Thicker ice with snow cover, like pack ice, has a lower surface temperature and has in general a higher

TCD
5, 3259–3289, 2011

albedo in comparison to very thin, dark nilas ice which can be found in the polynya region and on just-frozen leads. This thin ice, without snow cover, shows relatively warm temperatures near the freezing point and a low albedo. Perovich and Grenfell (1981) showed in laboratory experiments that when young sea ice like nilas becomes thicker the albedo increase fast. The reason is that with the decrease in ice temperature the amount of brine in the sea ice change as well which cause a change in its radiative properties.

Based on our observations of the sea surface conditions, for this study we classify sea ice areas adjacent to the Antarctic Peninsula into three main categories: we define as the first main sea ice area the North-Eastern Bellingshausen Sea where new, young and first year sea ice prevails. Our second main sea ice area is the Western Weddell Sea area, where multi-year pack ice eastward of, and adjacent to, the Larsen Ice Shelf persists. Our third area is defined as the southern part of the Western Weddell Sea, adjacent to the Ronne Ice Shelf, which has mainly a new, young first year sea ice cover in the Ronne Polynya area.

3.2 Mean albedo

In order to define characteristic surface values for these three main sea ice areas, we determined on the basis of the high resolution data for each flight mission the averaged sea surface albedo $\overline{\alpha}$ (albedo averaged over the entire surface) and sea ice albedo $\overline{\alpha_i}$ (albedo averaged over ice-covered areas only) and their corresponding temperatures $\overline{T_s}$ and $\overline{T_i}$, respectively. They are listed in Table 1. Four flights over the North-Eastern Bellingshausen Sea ice area, eleven flights over the Western Weddell Sea pack ice area and five flights over first year sea ice in the southern part of the Western Weddell Sea form the basis of this study. Our data show that the sea ice concentration in the Weddell Sea was always very high during our observations, i.e. $C_{ice} \geq 95\,\%$ whereas in the North-Eastern Bellingshausen Sea the sea ice concentrations showed also lower values and we observed $C_{ice} \geq 73\,\%$. The mean sea ice albedo which we observed in the Bellingshausen Sea, averaged over an entire flight, ranged from $\overline{\alpha_i} = 0.25$ up

TCD
5, 3259–3289, 2011

Albedo of the ice-covered Weddell and Bellingshausen Sea

A. I. Weiss et al.

to $\overline{\alpha_i} = 0.69$. In the Weddell Sea pack ice areas, we observed higher mean area-averaged sea ice albedo values, ranging from $\overline{\alpha_i} = 0.66$ up to $\overline{\alpha_i} = 0.82$. In contrast to this, we observed the smallest mean sea ice albedo values in the southern part of the Western Weddell Sea, where the mean area-averaged albedo ranged from $\overline{\alpha_i} = 0.24$ to $\overline{\alpha_i} = 0.42$. Figure 3 shows mean albedo and mean sea surface temperature $\overline{T_s}$ (water and sea ice) as function of mean sea ice concentration, averaged for each flight mission for the three different sea ice areas, as listed in Table 1. The mean albedo and sea surface temperature shows in our data set no clear dependence with mean sea ice concentration in none of the three sea ice areas. This can be explained by the fact, that our observations were collected over very compact sea ice cover. Other studies showed that with decrease in sea ice cover and increase water fraction the sea ice albedo decreases. This was shown by Brandt et al. (2005). They showed on the basis of satellite data that if the ice is pushed northward by the winds and currents so that there is a substantial fraction of open water on the sea surface the main determinant of area averaged albedo become the ice concentration.

Figure 4 displays for the three sea ice areas the percentage of sea surface within a given albedo bin ($\Delta\alpha = 0.1$) in the North-Eastern Bellingshausen Sea, the Western Weddell Sea and South-Western Weddell Sea. These distribution functions show that in all three sea ice areas we observed a wide range of albedo values, suggesting that all three areas contain a mixture of different sea ice types or mixture of sea ice of different age, snow cover and thickness. In the North-Eastern Bellingshausen Sea we observed that over 30 % of the sea surface had an albedo value which was less than 0.1, i.e. over 30 % of the surface was sea ice free or covered with newly-formed sea ice and dark nilas. In the South-Western Weddell Sea polynya region we observed a similar high percentage of small albedo values below 0.1 (app. 27 %), which indicates water or dark new ice. The Weddell Sea pack ice region showed, in contrast, less than 1 % of the surface with an albedo less than 0.1, indicative of open water or thin dark ice. In the pack ice area we observed that more than 80 % of the surface showed albedo values larger than 0.6, which is a typical value for thick, snow-covered sea ice.

TCD
5, 3259–3289, 2011

4 Discussion

4.1 Impact of mean albedo for numerical model studies

The knowledge of the mean area-averaged surface albedo can be used to improve numerical model simulations of these areas. Large-scale general circulation models often use a very simple albedo parameterization, which assumes a characteristic surface albedo value within the model grid box. Some models determine the ice cover within each model grid box and two characteristic albedo values are used, one for the prevailing sea ice type and the second one for open water. With a weighting function the mean albedo in the grid box is determined. There are also models which assume one albedo value for a model grid box, e.g. a value which is a mean of all albedo values within the grid box. Such a relative simple albedo parameterization approach is found for example in the large-scale sea ice model of Parkinson and Washington (1979), in the atmospherically forced sea ice model of Hibler and Bryan (1987), and the thermodynamic sea ice model of Ross and Walsh (1987), among others. Some models assume a characteristic albedo value for certain sea ice type. This approach is used e.g. in the sea ice model of Mellor and Kantha (1989). Lists of typical albedo values of certain sea ice types in Antarctica are given e.g. by Brandt et al. (2005) and Allison et al. (1993). In some models the sea surface albedo is not parameterized but is a prognostic variable, e.g. in the Goddard Institute for Space Studies (GISS) climate model as described by Hansen et al. (1983), in which the albedo is determined from the albedo value of the previous month. Whether assuming an albedo value or using a prognostic albedo value, both approaches for describing the sea surface albedo have in common that one mean albedo value is used within a grid box. In Table 2 we determined for the three defined main sea ice areas adjacent to the Antarctic Peninsula from the data listed in Table 1 mean albedo values. We calculated on the one hand mean albedo values for the sea surface which is composed of open water and sea ice, and on the other hand mean albedo values for ice-covered surface only, i.e. excluding the open water fraction. The corresponding mean percentage of sea ice cover is also

TCD
5, 3259–3289, 2011

listed in Table 2. Comparing the averaged albedo values for the sea surface consisting of a mixture of water and sea ice to the averaged albedo of the mixture of sea ice without water fraction, the values differ only slightly. The main reason for this is that we conducted our measurement over sea surfaces which show relatively high sea ice concentration in all three sea ice areas. We observed the largest mean sea ice albedo value of $\overline{\alpha_\mathrm{i}} = 0.75$ in the Western Weddell Sea pack ice area and the smallest mean albedo value of $\overline{\alpha_\mathrm{i}} = 0.38$ south of the pack ice area in the polynya region of the Weddell Sea, where young, new sea ice prevailed. In the North-Eastern Bellingshausen Sea we determined a characteristic mean sea ice albedo of $\overline{\alpha_\mathrm{i}} = 0.64$ from our data set.

4.2 Relation between albedo and temperature

Due to the fact that the sea ice albedo shows a tendency to increase with decreasing temperature some numerical models parameterize the albedo with the temperature as the only driving input parameter. An example for a model which predicts the sea surface albedo by a parameterization which uses the simulated surface temperature as only input parameter is the UK Met Office general circulation model, as described by Ingram et al. (1989). Ross and Walsh (1987) investigated with a dynamic-thermodynamic sea ice model the temperature dependence of snow and ice albedo for the Arctic. For their study they modified the Goddard Institute for Space Studies GISS sea ice model of Hansen et al. (1983), by using a temperature dependent albedo parameterization for snow and ice rather than a constant albedo value. The sea surface albedo parameterization of Køltzow (2007) uses also the temperature for the prediction of the albedo but can also take the influence of melt pond fraction on the sea surface albedo into account. This parameterization was determined from data measured in the Arctic sea ice zone for the Arctic HIRHAM model (Christensen et al., 1996). In the thermodynamic sea ice model described by Ledley (1985) the air temperature, and not the surface temperature, is used to parameterize the sea surface albedo. The parameterizations used in these models are listed in Table 3. To investigate whether one of these albedo parameterizations describes the sea ice albedo in the Bellingshausen or Weddell Sea

TCD
5, 3259–3289, 2011
Albedo of the ice-covered Weddell and Bellingshausen Sea
A. I. Weiss et al.

realistically, we compared them to our measurements. For this purpose, we determined a mean albedo value for surface temperature bins of $\Delta T_s = 1\,^{\circ}$C for each flight. We averaged the binned albedo for all flights within each of the three sea ice areas. The averaged relations for each sea ice area are shown in the upper panels of Fig. 5 for temperatures below the freezing point. All three panels in Fig. 5 verify the tendency for the mean sea ice albedo to increase with decreasing surface temperature. In the lower panels of Fig. 5 we display the number of data points which were available within each temperature bin. This gives an indication of the mixture of different sea surface temperatures which we observed in the three sea ice areas adjacent to the Antarctic Peninsula. In the North-Eastern Bellingshausen Sea the first year ice shows temperatures between the freezing point and about $T_i = -8\,^{\circ}$C, but most observations in the Bellingshausen Sea showed surface temperatures around $T_i = -3\,^{\circ}$C. In the Weddell Sea ice areas a much larger surface temperature range was observed, ranging from the freezing point to temperatures $T_i \leq -14\,^{\circ}$C.

In Fig. 6 we compare the three examples of albedo parameterization schemes that we listed in Table 3 with our bin-averaged albedo observations for the three sea ice areas. Each albedo parameterization scheme which is shown in Fig. 6 covers a different surface temperature interval and each scheme show a different function with decreasing temperature. Comparing the parameterizations with our data it is seen that the parameterization of Køltzow (2007) overestimates the sea surface albedo in the North-Eastern Bellingshausen Sea, as well as in the Weddell Sea pack ice and new, young sea ice area. This parameterization was developed on the basis of Arctic sea ice. The parameterization of Ross and Welsh (1987) overestimates the sea surface albedo of the North-Eastern Bellingshausen Sea as well as of the Southern Weddell Sea, however the high albedo values in the pack ice area of the Western Weddell Sea are captured well by this parameterization. The model parameterization which is described by Ingram et al. (1989) overestimates the new/young sea ice area albedo that we observed in the South-Western Weddell Sea, but the predicted albedo values capture better the values of the first year sea ice in the North-Eastern Bellingshausen

TCD
5, 3259–3289, 2011
Albedo of the ice-covered Weddell and Bellingshausen Sea
A. I. Weiss et al.

Sea and the albedo values which we observed in the pack ice area in the Weddell Sea. Summing up, the albedo data observed in the new/young sea ice area are not very well captured by any of the parameterizations tested. In this area the sea ice was characterized with hardly any snow cover so that sea ice albedo depends mainly on the ice types, its age and/or thickness.

Summing up, the biggest differences which we see between parameterizations and the measurements are in the areas where thin, young ice prevails. This is probable because most albedo parameterization were developed on the basis of measurements over thick consolidated ice. In situ measurements over thin ice are still rare. A further reason for the differences in values between the predicted albedo and the observed albedo in the sea ice areas adjacent to the Antarctic Peninsula could be that most parameterizations are not accounting for such a large variety and mixture of sea ice types. Moreover, the parameterizations are often developed on the basis of Arctic sea ice measurements, so they are probably accounting for Arctic physical sea ice processes which may not be important in the Antarctic sea ice zone. Most fundamental differences between Arctic and Antarctic sea ice result from the geographic differences between the two regions, which have an influence on the sea surface albedo. For example, in the Arctic there is only a small fraction of ice advected out of the area and there is less annual variability. In the Antarctic the sea ice can be transported by wind and ocean current northwards which increases the water fraction of the sea ice areas and enhanced the melt processes and decrease the sea surface albedo (Brandt et al., 2005). In the Antarctic frazil crystals in open water make a major contribution to the total ice mass, and the dynamic processes of rafting and ridging are the main mechanisms for the ice growth and thickness changes. The amount of impurities (e.g. black carbon, mineral dust or volcanic ash) on sea ice differs between Arctic and Antarctic as well as biological processes in the sea ice. In general, impurities lower the albedo of snow-covered surfaces, which is described for black carbon by Jacobson (2004). A further example for a physical sea ice process which differs in the Arctic from the Antarctic is the melting process of the ice. In the Arctic extensive melt ponds can be

TCD
5, 3259–3289, 2011

observed on sea ice during summer (Perovich et al., 2002), which are not presences in the Antarctic. The inclusion of melt ponds in the albedo scheme is therefore important for the Arctic sea ice areas because the melt ponds absorb a large portion of solar energy (Pedersen et al., 2009). Melt ponds are hardly observed on Antarctic sea ice, which gives the motivation to exclude from our comparison a melt pond parameterization. There still exists in all the examples, which are shown in Fig. 6, for certain temperature bins relatively large differences in predicted and measured albedo values. We determined from bin-averaged albedo and temperature values, shown in Fig. 5, linear temperature/albedo functions for the three defined sea ice areas adjacent to the Antarctic Peninsula. We defined these functions between a maximum and minimum albedo value. As a minimum value we use the freezing temperature of the sea ice area and as the maximum value we use the maximum value from the averaged sea surface temperature data. This temperature albedo functions are listed also in Table 3.

5 Summary and concluding remarks

The aircraft data of this study showed that the sea ice areas adjacent to the Antarctic Peninsula consist of a mixture of different sea ice types with a large range of albedo values. Each compact sea ice area is characterized by a different mixture of certain ice types, but all sea ice areas show values over the entire sea ice albedo range from 0.07 to more than 0.8 in summer. The North-Eastern Bellingshausen Sea ice area is characterized by a mixture mainly of first year ice, the Western Weddell Sea by mainly of multi-year pack ice with leads, with the exception of the south-western part, where a mixture of new, young sea ice prevailed. The observations showed that a characteristic area-averaged sea ice albedo value, which is needed for example as boundary parameter for a model grid box, should be an average albedo value of different sea ice types, weighted with their frequency distribution. We determined frequency distributions of sea ice albedo values and of averaged albedo values (Table 2) for the three sea ice areas adjacent to the Antarctic Peninsula in summer from aircraft measurements.

TCD
5, 3259–3289, 2011

Previous studies showed that various factors influence the ice and snow albedo, but commonly only the sea surface temperature is used to parameterize the albedo in climate and weather prediction models. The reason for this is that the temperature is relatively easy available as input parameter in all models and the temperature is a good proxy for various factors influencing the radiative properties of sea ice. This gives the motivation to investigate the relation of albedo with temperature in the sea ice areas adjacent to the Antarctic Peninsula. We compared the aircraft albedo data with published linear temperature albedo parameterizations. In particular the albedo of areas with new, young ice, which we observed in the southern part of the Weddell Sea, was over predicted by all tested parameterizations. Summing up, the comparison showed that not one linear parameterization can predict the albedo of all three sea ice areas adjacent to the Antarctic Peninsula, with sufficient accuracy. One reason for this might be that the temperature can act as a proxy for different factors which influences the radiative properties of sea ice. One the one hand the temperature can act as proxy mainly for the ice thickness and one the other hand mainly for the conditions of the snow-cover on sea ice. For thin bare, new and young sea ice, which we observed in particular in the polynya region and on just-frozen leads, the sea ice albedo is mainly influenced by the sea ice thickness. We observed a rapid increase of the albedo with increase in sea ice thickness, i.e. decrease in temperature, but the albedo values are lower than those of sea ice which has the same temperature but which is snow-covered. On the other hand the data showed that the albedo of snow-covered sea ice was generally much larger than that of snow-free ice and increases more slowly with decreasing temperature. This indicates that for snow-covered sea ice the temperature acts in particular as a proxy for the snow conditions and snow metamorphosis, the sea ice thickness becomes less important. Commonly used parameterizations use the surface temperature as proxy in particular for the snow cover and metamorphosis on the ice and not as proxy for the ice thickness, which is most important for thin, new sea ice. Summing up, the study shows that one linear temperature albedo parameterization can be only a rough approximation for sea ice areas which show a mixture of bare

TCD
5, 3259–3289, 2011

and snow-covered sea ice. We observed such a mixture of bare and snow-covered sea ice in all three sea ice areas adjacent to the Antarctic Peninsula, but with various frequency distributions of ice types. We determined typical linear temperature-albedo functions for three sea ice areas adjacent to the Antarctic Peninsula from the aircraft data, which are listed in Table 3.

The large number of factors which influence the radiative properties of sea ice implies that for a more accurate albedo parameterization, further input parameters should be taken into account and have to be available as input parameters within the model. There is in particular a need for a better parameterization of the albedo over thin/new sea ice. Such parameterization will be particularly important as model resolution increases and as models are able to resolve features such as large polynyas, where thin ice prevails. More sophisticated model parameterizations do already exists in complex sea ice models. They use as input parameter not only the temperature, but also the ice thickness (e.g. Manabe et al., 1992; Flato and Brown, 1996) and snow cover of ice, e.g. in the Arctic regional climate system model (ARCSYM) described by Lynch et al. (1995). However, for a determination or validation of such complex albedo parameterization further area-covering observations of additional surface parameters, like averaged sea ice thickness and snow conditions have to be conducted in the sea ice areas of the Antarctic Peninsula.

References

Allison, I., Brandt, R. E., and Warren, S. G.: East Antarctic sea ice: albedo, thickness distribution, and snow cover, J. Geophys. Res., 98, 12417–12429, 1993.

Bannehr, L. and Glover, V.: Preprocessing of airborne Pyranometer data, NCAR Technical Note 364, 1–35, 1991.

Brandt, R. E., Warren, S. G., Worby, A. P., and Grenfell, T. C.: Surface albedo of the Antarctic sea ice zone, J. Climate, 18, 3606–3622, 2005.

Bracegirdle, T. J., Connolley, W. M., and Turner, J.: Antarctic climate change over the twenty first century, J. Geophys. Res., 113, D03103, doi:10.1029/2007JD008933, 2008.

Discussion Paper | Discussion Paper | Discussion Paper | Discussion Paper |

TCD

5, 3259–3289, 2011

Albedo of the ice-covered Weddell and Bellingshausen Sea

A. I. Weiss et al.

Burns, S. P., Khelif, D., Friehe, C. A., Hignett, P., Williams, A. G., Grant, A. L. M., Hacker, J. M., Hagan, D. E., Serra, Y. L., Rodgers, D. P., Bradley, E. F., Weller, R. A., Fairall, C. W., Anderson, S. P., Paulson, C. A., and Coppin, P. A.: Comparison of aircraft, ship, and buoy radiation and SST measurements from TOGA COARE, J. Geophys. Res., 105(D12), 15627–15652, 2000.

Christensen, J. H., Christensen, O. B., Lopez, P., van Meijgaard, E., and Botzet, M.: The HIRHAM4 Regional Atmospheric Climate Model, Scientific Report, Danish Meteorological Institute, Copenhagen, 1996.

Curry, J. A., Schramm, J., Perovich, D. K., and Pinto, J. O.: Applications of SHEBA/FIRE data to evaluation of snow/ice albedo parameterizations, J. Geophys. Res., 106(D14), 15345–15355, 2001.

Flato, G. M. and Brown, R. D.: Variability and climate sensitivity of landfast Arctic sea ice, J. Geophys. Res., 101, 25767–25777, 1996.

Grenfell, T. C. and Perovich, D. K.: Spectral albedos of sea ice and incident solar irradiance in the Southern Beaufort Sea, J. Geophys. Res., 89(C3), 3573–3580, 1984.

Grenfell, T. C., Warren, S. G., and Mullen, P. C.: Reflection of solar radiation by the Antarctic snow surface at ultraviolet, visible and near-infrared wavelengths, J. Geophys. Res., 99, 18669–18684, 1994.

Hansen, J., Russell, G., Rind, D., Stone, P., Lacis, A., Lebedeff, S., Ruedy, R., and Travis, L.: Efficient three-dimensional global models for climate studies: models I and II, Mon. Weather Rev., 111, 609–662, 1983.

Hibler III, W. D. and Bryan, K.: A diagnostic ice-ocean model, J. Phys. Oceanogr., 17(7), 987–1015, 1987.

Ingram, W. J., Wilson, C. A., and Mitchell, J. F. B.: Modeling climate change: an assessment of sea ice and surface albedo feedbacks, J. Geophys. Res., 94, 8609–8622, 1989.

Jacobson, M. Z.: Climate response of fossil fuel and biofuel soot, accounting for soot's feedback to snow and sea ice abledo and emissivity, J. Geophys. Res., 109, D21201, 15 pp., doi:10.1029/2004JD004945, 2004.

Jenkins, A. and Jacobs, S.: Circulation and melting beneath George VI Ice Self, Antarctica, J. Geophys. Res., 113, C04013, doi:10.1029/2007JC004449, 2008.

King, J. C., Lachlan-Cope, T. A., Ladkin, R. S., and Weiss, A.: Airborne measurements in a stable boundary layer over the Larsen Ice Shelf, Antarctica, Bound.-Lay. Meteorol., 127, 413–428, 2008.

Køltzow, M.: The effect of a new snow and sea ice albedo scheme on regional climate model simulations, J. Geophys. Res., 112, DO7110, 12 pp., doi:10.1029/2006JD007693, 2007.

Ledley, T.: Sensitivity of a thermodynamic sea ice model with leads to time step size, J. Geophys. Res., 90(D1), 2251–2260, 1985.

Liu, J., Curry, J. A., and Martinson, D. G.: Interpretation of recent Antarctic sea ice variability, Geophys. Res. Lett., 31, L02205, doi:10.1029/2003GL018732, 2004.

Lynch, A. H., Chapman, W. L., Walsh, J. E., and Weller, G.: Development of a regional climate model of the Western Arctic, J. Climate, 8, 1555–1570, 1995.

Manabe, S., Spelman, M. J., and Stouffer, R. J.: Transient responses of a coupled ocean-atmosphere model to gradual changes of atmospheric CO_2. Part II: Seasonal response, J. Climate, 5, 105–126, 1992.

Mellor, G. L. and Kantha, L.: An ice-ocean coupled model, J. Geophys. Res., 94, 10937–10954, 1989.

Nicholls, K. W., Østerhus, S., Makinson, K., and Johnson, M. R.: Oceanographic conditions south of Berkner Island, beneath Filchner–Ronne Ice Shelf, Antarctica, J. Geophys. Res., 106, 11481–11492, 2001.

Nicholls, K. W., Boeme, S. L., Biuw, M., and Fedak, M. A.: Wintertime ocean conditions over the Southern Weddell Sea continental shelf north of Ronne Ice Shelf, Antarctica, Geophys. Res. Lett., 35, L21605, doi:10.1029/2008GL035742, 2008.

Parkinson, C. L. and Washington, W. M.: A large-scale numerical model of sea ice, J. Geophys. Res., 84, 311–337, 1979.

Pedersen, C. A., Roeckner, E., Luethje, M., Winther, J.-G.: A new sea ice albedo scheme including melt ponds for ECHAM5 general circulation model, J. Geophys. Res., 114, DO8101, doi:10.1029/2008JD010440, 2009.

Perovich, D. K. and Grenfell, T. C.: Laboratory studies of the optical properties of young sea ice, J. Galciology, 27, 331–346, 1981.

Perovich, D. K., Tucker III, W. B., and Ligett, K. A.: Aerial observation of the evolution of ice surface conditions during summer, J. Geophys. Res., 107, 8048, doi:10.1029/2000JC000449, 2002.

Pirazzini, R.: Surface albedo measurements over Antarctic sites in summer, J. Geophys. Res., 109, D20118, 2004.

Predoehl, M. C. and Spano, A. F.: Airborne albedo measurements over the Ross Sea, October–November 1962, Mon. Weather Rev., 93, 687–696, 1965.

Ross B. and Walsh, J. E.: A comparison of simulated and observed fluctuations in summertime Arctic surface albedo, J. Geophys. Res., 92, 13115–13125, 1987.
Turner, J., Lachlan-Cope, T. A., Colwell, S. T., and Marshall, G. J.: Significant warming of the Antarctic winter troposphere, Science, 311(5769), 1914–1917, 2006.
Vashisth, P.: Effect of clouds and free water on snow albedo, Bull. Glaciol. Res., 22, 63–67, 2005.
Vihma, T., Johansson, M. M., and Launiainen, J.: Radiative and turbulent surface heat fluxes over sea ice in the Western Weddell Sea in early summer, J. Geophys. Res., 114, C04019, doi:10.1029/2008JC004995, 2009.
Weiss, A. I., King, J. C., Lachlan-Cope, T. A., and Ladkin, R.: On the effective aerodynamic and scalar roughness length of Weddell Sea ice, J. Geophys. Res., 116, D19119, doi:10.1029/2011JD015949, 2011.
Wiscombe, W. J. and Warren, S. G.: A model of the spectral albedo of snow, I: pure snow, J. Atmos. Sci., 37, 2712–2733, 1980.
Zhou, X., Li, S., Morris, K., and Jeffries, M. O.: Albedo of summer snow on sea ice, Ross Sea, Antarctica, J. Geophys. Res., 112, D16105, doi:10.1029/2006JD007907, 2007.

TCD
5, 3259–3289, 2011

Table 1. Time and location of flight missions in the Weddell and Bellingshausen Sea, median surface temperature $\overline{T}_s$, sea ice temperature $\overline{T}_i$, water temperature $\overline{T}_w$, ice concentration C_{ice}, water fraction (as concentration) C_w, surface albedo $\overline{\alpha}$, sea ice albedo $\overline{\alpha_i}$, and sea water albedo $\overline{\alpha_w}$ are listed for each flight mission with their standard deviations σ.

NE Bellingshausen Sea (first year ice)	Date	Flight length (km)	Ice and water $\overline{T}_s \pm \sigma_T$ (°C)	$\overline{\alpha} \pm \sigma_\alpha$	C_{ice} (%)	Sea ice only $\overline{T}_i \pm \sigma_T$ (°C)	$\overline{\alpha}_i \pm \sigma_\alpha$	C_w (%)	Water only $\overline{T}_s \pm \sigma_T$ (°C)	$\overline{\alpha}_w \pm \sigma_\alpha$
69.38° S 72.80° W to 70.59° S 75.63° W	13 Feb 07	396	−0.61 ± 0.44	0.63 ± 0.20	91	−0.6 ± 0.43	0.65 ± 0.14	9	−1.09 ± 0.39	0.06 ± 0.01
69.48° S 73.08° W to 69.95° S 74.39° W	21 Feb 07	176	−3.23 ± 0.93	0.68 ± 0.21	88	−3.33 ± 0.59	0.69 ± 0.09	12	0.89 ± 0.21	0.07 ± 0.01
69.31° S 72.97° W to 69.69° S 75.03° W	21 Feb 07	171	−2.54 ± 0.79	0.63 ± 0.09	100	−2.54 ± 0.79	0.63 ± 0.09	0	No open water	No open water
68.61° S 70.84° W to 69.49° S 72.24° W	26 Feb 07	634	−2.3 ± 2.27	0.16 ± 0.22	73	−2.91 ± 2.41	0.25 ± 0.2	27	−0.87 ± 0.62	0.07 ± 0.05
W Weddell Sea (pack ice)										
68.71° S 60.66° W to 69.12° S 58.16° W	15 Feb 07	365	−8.94 ± 1.44	0.80 ± 0.05	100	−8.94 ± 1.44	0.80 ± 0.05	0	No open water	No open water
70.09° S 61.45° W to 71.65° S 59.26° W	16 Feb 07	327	−8.09 ± 2.09	0.75 ± 0.16	100	−8.09 ± 2.09	0.75 ± 0.16	0	No open water	No open water
69.35° S 61.30° W to 70.78° S 58.66° W	16 Feb 07	212	−6.93 ± 1.49	0.76 ± 0.16	< 100	−6.94 ± 1.49	0.76 ± 0.16	> 0	−1.75 ± 0.01	0.08 ± 0.00
66.90° S 60.77° W to 67.44° S 55.92° W	01 Mar 07	387	−12.27 ± 2.79	0.81 ± 0.17	< 100	−12.38 ± 2.70	0.82 ± 0.19	> 0	−0.59 ± 0.17	0.09 ± 0.0
67.35° S 61.14° W to 67.71° S 57.54° W	29 Jan 08	257	−1.89 ± 0.57	0.68 ± 0.10	99	−1.89 ± 0.57	0.68 ± 0.09	1	−1.10 ± 0.26	0.1 ± 0.0
66.71° S 60.17° W to 66.09° S 57.88° W	02 Feb 08	459	−0.92 ± 0.30	0.69 ± 0.12	< 100	−0.92 ± 0.32	0.69 ± 0.12	> 0	−1.75 ± 0.05	0.06 0.01
73.96° S 59.00° W to 69.92° S 59.29° W	09 Feb 08	563	−3.83 ± 0.76	0.77 ± 0.13	98	−4.58 ± 0.13	0.79 ± 0.02	2	−1.77 ± 0.1	0.09 0.0
69.88° S 59.21° W to 65.24° S 59.22° W	10 Feb 08	538	−2.15 ± 0.63	0.74 ± 0.10	99	−2.60 ± 0.12	0.75 ± 0.01	1	−1.78 ± 0.04	0.09 ± 0.01
65.15° S 58.95° W to 66.23° S 59.10° W	18 Feb 08	181	−1.5 ± 0.53	0.65 ± 0.17	95	−1.53 ± 0.54	0.66 ± 0.12	5	−1.2 ± 0.17	0.06 ± 0.01
68.00° S 60.98° W to 67.64° S 55.00° W	21 Feb 08	277	−5.68 ± 0.99	0.74 ± 0.11	100	−5.68 ± 0.99	0.74 ± 0.11	0	No open water	No open water
68.00° S 60.98° W to 67.64° S 55.00° W	21 Feb 08	312	−7.72 ± 1.78	0.73 ± 0.18	100	−7.72 ± 1.78	0.73 ± 0.18	0	No open water	No open water
SW Weddell Sea new, (young sea ice)										
75.04° S 60.25° W to 74.58° S 58.10° W	25 Feb 07	164	−6.31 ± 1.95	0.38 ± 0.20	100	−6.61 ± 1.97	0.38 ± 0.29	0	−1.76 ± 0.05	0.09 ± 0.00
74.20° S 59.31° W to 74.83° S 61.01° W	27 Feb 07	265	−12.32 ± 2.89	0.41 ± 0.12	100	−12.32 ± 2.89	0.41 ± 0.12	0	No open water	No open water
74.98° S 60.69° W to 74.11° S 57.68° W	28 Feb 07	85	−10.68 ± 2.71	0.42 ± 0.10	100	−10.68 ± 2.71	0.42 ± 0.10	0	No open water	No open water
74.58° S 61.23° W to 74.36° S 58.59° W	05 Feb 08	350	−5.77 ± 2.71	0.24 ± 0.29	99	−5.78 ± 2.78	0.24 ± 0.29	1	−1.82 ± 0.05	0.06 ± 0.01
75.04° S 60.30° W to 74.51° S 57.61° W	06 Feb 08	104	−3.56 ± 3.41	0.29 ± 0.27	< 100	−3.57 ± 3.4	0.29 ± 0.27	> 0	−0.44 ± 0.10	0.09 ± 0.01

TCD
5, 3259–3289, 2011

Table 2. Averaged sea surface and sea ice albedo of data listed in Table 1 for the North-Eastern Bellingshausen Sea, Western Weddell Sea and South-Western Weddell Sea with average percentage of sea ice cover.

	NE Bellingshausen Sea first year sea ice area	W Weddell Sea pack ice area	SW Weddell Sea new or young sea ice area
$\overline{\alpha} \pm \sigma_\alpha$ sea surface (mix of sea ice and open water)	0.63 ± 0.24	0.74 ± 0.05	0.38 ± 0.12
$\overline{Ts} \pm \sigma_{Ts}$ sea surface (mix of sea ice and open water)	$-2.4 \pm 1.10\,^\circ$C	$-5.6 \pm 3.64\,^\circ$C	$-6.31 \pm 3.91\,^\circ$C
Average percentage of sea ice cover	89.2 %	99.9 %	99.9 %
$\overline{\alpha}_\mathrm{i} \pm \sigma_\alpha$ (mix of sea ice without open water)	0.64 ± 0.20	0.75 ± 0.05	0.38 ± 0.08
$\overline{T}_i \pm \sigma_{Ti}$ (mix of sea ice without open water)	$-2.72 \pm 1.2\,^\circ$C	$-5.68 \pm 3.63\,^\circ$C	$-6.61 \pm 3.61\,^\circ$C

TCD
5, 3259–3289, 2011

Table 3. Model temperature-albedo parameterizations with T_s = surface temperature, T_a = air temperature and averaged linear temperature-albedo relations of this study, determined for the North-Eastern Bellingshausen Sea covered with first year ice, the Western Weddell Sea pack ice area and the southern part of the Western Weddell Sea ice area covered with new/young ice.

Reference (or origin) of albedo parameterization	Albedo parameterization schemes for sea ice or ice-covered sea surface	Temperature range for which the parameterization is valid
UK Met Office GCM Ingram et al. (1989)	$\alpha = 0.7$ $\alpha = 0.7 - 0.03 \cdot (T_s - 261.2)$ $\alpha = 0.4$	$T_s \leq 261.2\,\text{K}$ $261.2\,\text{K} < T_s < 271.2\,\text{K}$ $T_a = 271.2\,\text{K}$
Dynamic-thermodynamic sea ice model Ross and Walsh (1987) α_s = snow albedo α_i = ice albedo	$\alpha_s = 0.8$ $\alpha_s = 0.65 + 0.03 \cdot (-T_s)$ $\alpha_s = 0.65$ $\alpha_i = 0.65$ $\alpha_i = 0.45 - 0.04 \cdot T_a$ $\alpha_i = 0.45$	$T_s < -5\,^\circ\text{C}$ $-5\,^\circ\text{C} < T_s < 0\,^\circ\text{C}$ $T_s = 0\,^\circ\text{C}$ $T_s < 0\,^\circ\text{C}$ $0\,^\circ\text{C} < T_a < 5\,^\circ\text{C}$ $T_a = 5\,^\circ\text{C}$
Køltzow (2007) Version 1, without melt pond	$\alpha_i = 0.84$ $\alpha_i = 0.84 - 0.145 \cdot (2 + T_s)$ $\alpha_i = 0.51$	$T_a \leq -2\,^\circ\text{C}$ $0\,^\circ\text{C} > T_s > -2\,^\circ\text{C}$ $T_s \geq 0\,^\circ\text{C}$
Thermodynamic sea ice model Ledley (1985)	$\alpha_i = 0.88$ $\alpha_i = 0.88 - 0.00308 \cdot (T_a - 245)$ $\alpha_i = 0.79992 - 0.0322 \cdot (T_a - 271)$ $\alpha_i = 0.51$	$T_a \leq 245\,\text{K}$ $245\,\text{K} < T_a \leq 271\,\text{K}$ $271\,\text{K} < T_a \leq 280\,\text{K}$ $280\,\text{K} < T_a$
This study: North-Eastern Bellingshausen Sea, first year sea ice area with open water, Feb 2007	$\alpha_i = 0.07$ $\alpha_i = -0.0396 \cdot T_s + 0.4716$ $\alpha_i = 0.75$	$T_s > -1.84\,^\circ\text{C}$ $-1.84\,^\circ\text{C} \geq T_s \geq -7.035\,^\circ\text{C}$ $T_s < -7.035\,^\circ\text{C}$
This study: Western Weddell Sea, pack ice area with leads, Feb, Mar 2007 and Jan, Feb 2008	$\alpha_i = 0.07$ $\alpha_i = -0.0363 \cdot T_s + 0.406$ $\alpha_i = 0.87$	$T_s > -1.89\,^\circ\text{C}$ $-1.89\,^\circ\text{C} \geq T_s \geq -12.84\,^\circ\text{C}$ $T_s < -12.84\,^\circ\text{C}$
This study: South-Western Weddell Sea, new/young sea ice area with patches of open water, Feb 2007 and 2008	$\alpha_i = 0.07$ $\alpha_i = -0.0502 \cdot T_s + 0.0464$ $\alpha_i = 0.87$	$T_s > -1.87\,^\circ\text{C}$ $-1.87\,^\circ\text{C} \geq T_s \geq -16.58\,^\circ\text{C}$ $T_s - 16.58\,^\circ\text{C}$

TCD
5, 3259–3289, 2011

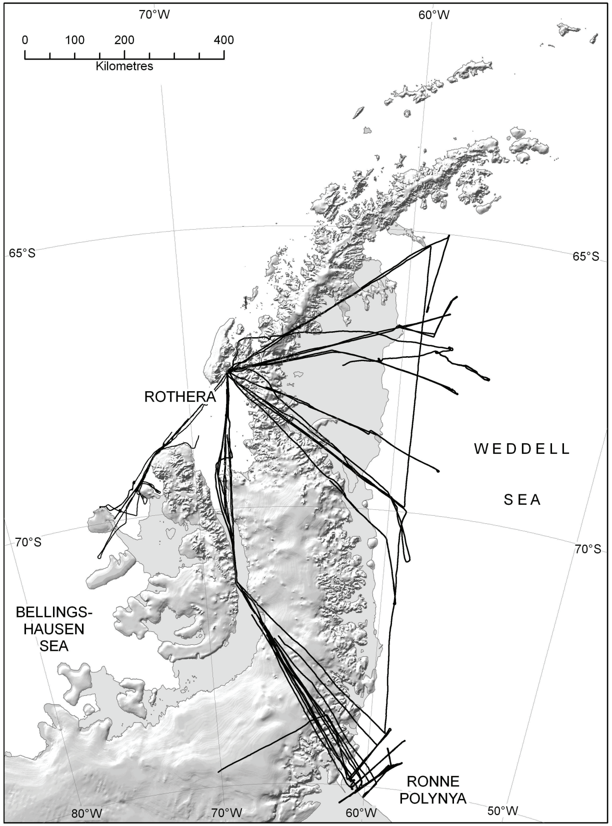

Fig. 1. Map of Antarctic Peninsula with flight tracks (black lines) flown during the aircraft field campaigns 2007 and 2008, which form the basis of this study.

TCD
5, 3259–3289, 2011

Albedo of the ice-covered Weddell and Bellingshausen Sea

A. I. Weiss et al.

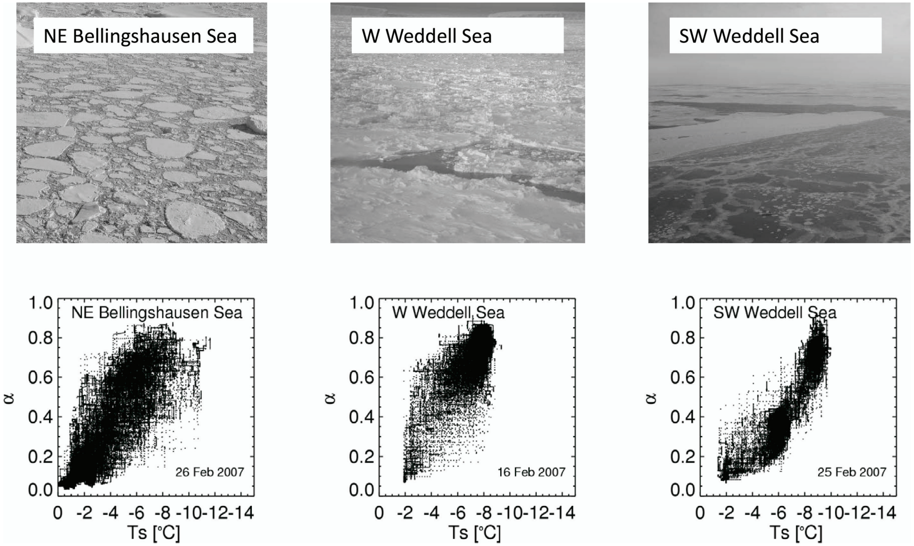

Fig. 2. Top panels show pictures of typical sea ice conditions during our field campaign in the North-Eastern Bellingshausen Sea (left panel), the Western Weddell Sea pack ice area (middle panel), and the South-Western Weddell Sea Ronne Polynya area (right panel). The lower panels show the corresponding albedo versus surface temperature (10 Hz high resolution data).

TCD
5, 3259–3289, 2011

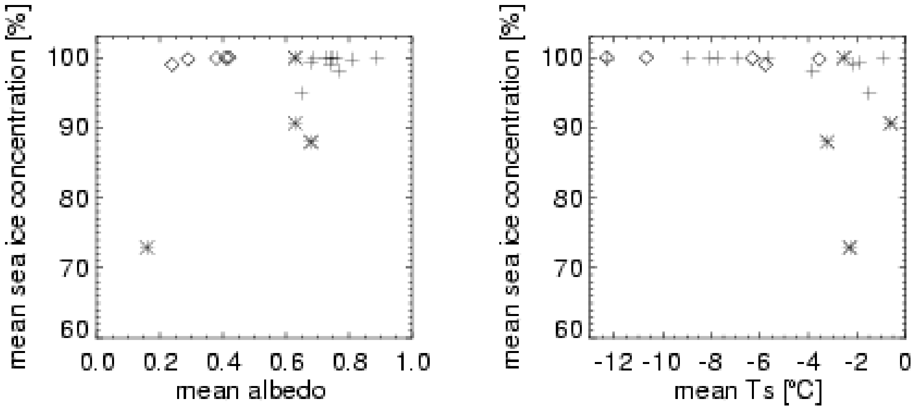

Fig. 3. Mean albedo (left panel) and mean sea surface temperature $\overline{T_s}$ (water and sea ice, right panel) as function of mean sea ice concentration, averaged for each flight mission, as listed in Table 1. The symbols represent the different sea ice areas: W Weddell Sea (plus sign), NE Bellingshausen Sea (asterisk), SW Weddell Sea (diamond).

TCD
5, 3259–3289, 2011

Albedo of the ice-covered Weddell and Bellingshausen Sea

A. I. Weiss et al.

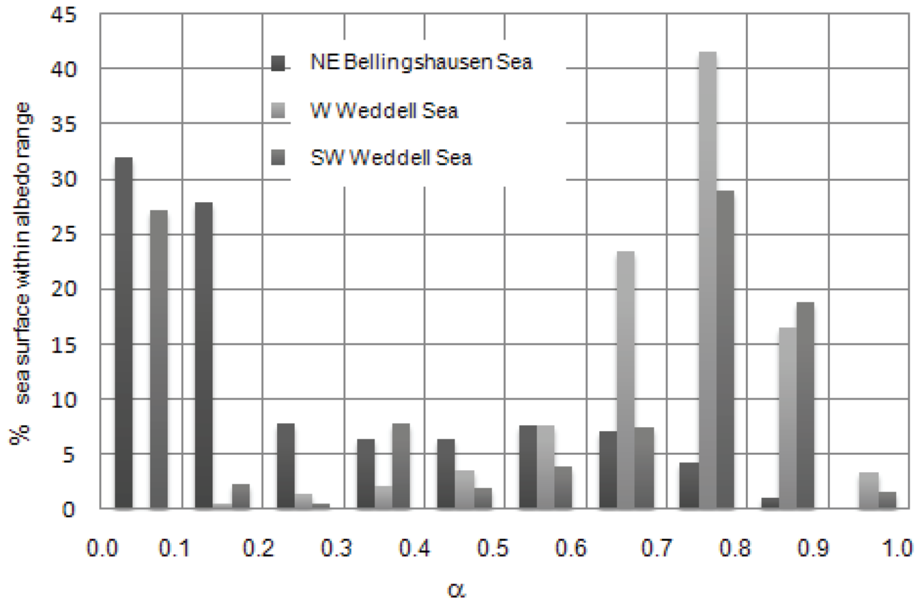

Fig. 4. Percentage of sea surface within a given albedo bin ($\Delta\alpha = 0.1$) in the North-Eastern Bellingshausen Sea, the Western Weddell Sea and South-Western Weddell Sea ice areas.

TCD
5, 3259–3289, 2011

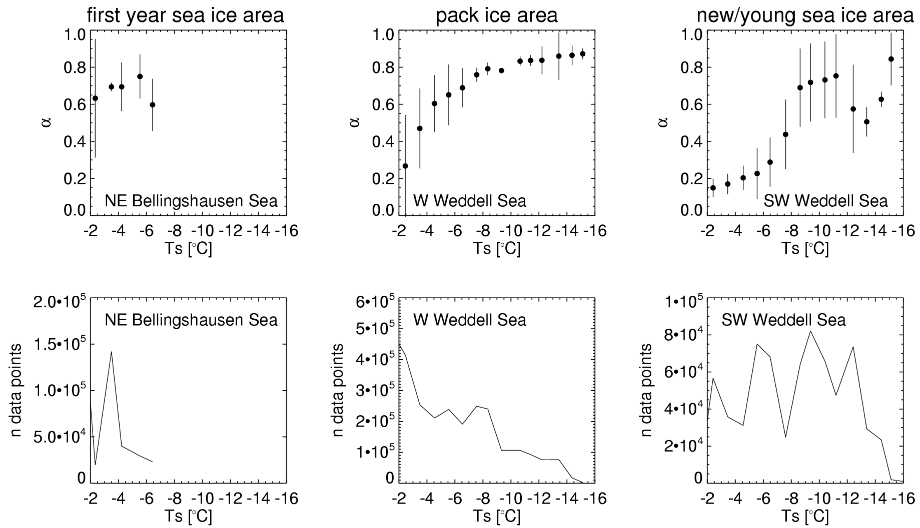

Fig. 5. From left to right, upper row: bin-averaged surface temperature values $\Delta T = 1\,^{\circ}\mathrm{C}$ below freezing point versus albedo of the sea surface measured in the North-Eastern Bellingshausen Sea covered mainly with first year ice, the Western Weddell Sea pack ice area and the southern part of the Western Weddell Sea ice area, covered mainly with new and young ice. Lower row shows number of data points with surface temperature.

TCD
5, 3259–3289, 2011

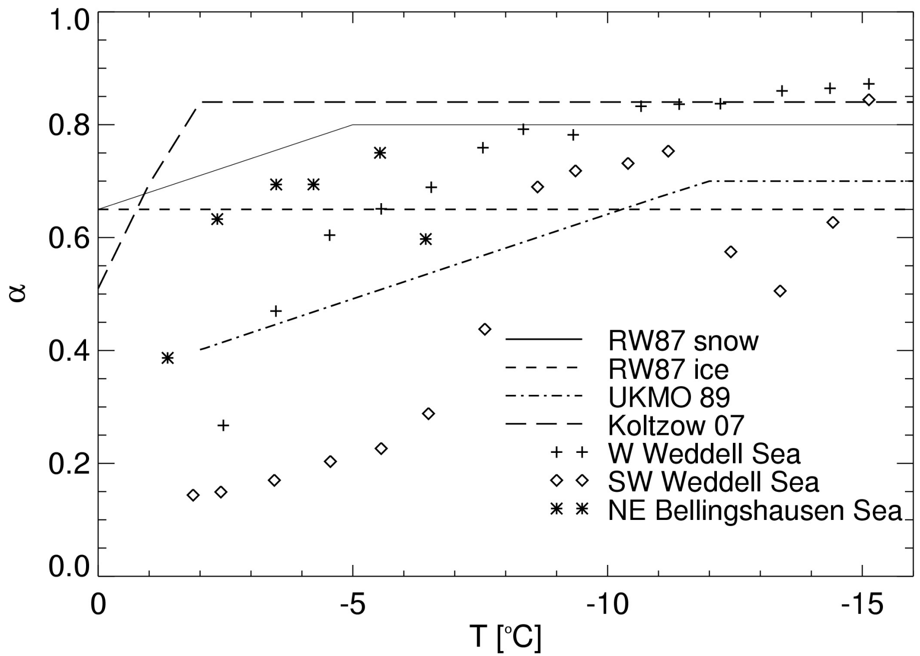

Fig. 6. Examples of albedo parameterization schemes, listed in Table 3, that use the surface temperature as driving input parameter: *RW87* shows the albedo parameterization scheme of Ross and Walsh (1987) for snow-covered and bare ice, respectively; *UKMO89* is the parameterization of the UK Met Office GC model, as described by Ingram et al. (1989) and *Koltzow 07* a parameterization scheme for the HIRHAM model (Christensen et al, 1996) which is described by Køltzow (2007), Version 1, i.e. with the assumption of no melt pond fraction. The parameterizations are shown only for temperatures below zero degrees. Additionally shown are the bin-averaged albedo data of this study for the Western Weddell Sea ice area, South-Western Weddell Sea ice area and North-Eastern Bellingshausen Sea in summer average over $\Delta T = 1\,^{\circ}\mathrm{C}$ temperatures bins.

TCD
5, 3259–3289, 2011